

Constrained deformation of a confined solid: a strain induced crystal-smectic transition

Debasish Chaudhuri and Surajit Sengupta
 Satyendra Nath Bose National Centre for Basic Sciences,
 Block-JD, Sector-III, Salt Lake, Calcutta - 700098.
 (Dated: December 1, 2018)

We report results of computer simulations of two-dimensional hard disks confined within a quasi one-dimensional “hard-wall” channel, a few atomic radii wide. Starting from a commensurate triangular solid a rescaling of the system size parallel to the channel length introduces a rectangular distortion of the solid which, beyond a critical limit, phase separates into alternating bands of solid and *smectic* phases. The resulting solid- smectic interfaces are broad and incorporate misfit dislocations. The stress-strain curve shows large plastic deformation accompanying the crystal-smectic transition which is reversible. The smectic phase eventually melts into a modulated liquid with a divergent Lindemann parameter.

Studies of small assemblages of molecules with one or more dimensions comparable to a few atomic spacings are significant in the context of nano-technology[1]. Designing nano-sized machines requires a knowledge of the mechanical behavior of systems up to atomic scales, where, a priori, there is no reason for continuum elasticity theory to be valid. In most cases, however, the effects of finite size are relatively mild, showing up mainly as a variation of the numerical value of the elastic constants[2] as a function of length scale. In this Letter, we show, on the other hand, that small size and hard constraints can produce essentially new phenomena without a counterpart in the bulk system. We perform computer simulations of the simplest possible, nontrivial, molecular system, namely, two-dimensional hard disk “atoms” confined within a quasi one-dimensional channel; the physics of which is entirely governed by geometry. Bulk hard disks in two dimensions are known to melt[3, 4, 6] from a high density triangular lattice to an isotropic liquid with a narrow intervening hexatic phase[5, 6]. In contrast, for channel widths of a few atomic spacings, we find evidence for a *smectic* phase which nucleates as prominent bands within the solid. The smectic phase arises when the size of the system in the direction parallel to the fixed walls is increased. A crystal to smectic transition, though predicted for anisotropic molecules[7] is unusual for hard disks – the anisotropy in this case arising purely from the external confining potential. In this respect, our results resemble the phenomenon of laser induced freezing[8] where an external modulated electric field produced by crossed laser beams induces a series of phase transitions[9, 10] involving triangular solid, modulated liquid as well as smectic phases. The analog of the modulating potential in our case is, of course, provided by the walls which induce a periodic potential of mean force[11, 12] decaying with distance from the walls. The nature of the crystal- smectic transition in our system, as we show below, are, however, different. Our results may be directly verified in experiments on sterically stabilized “hard sphere” colloids[13] confined in glass channels and

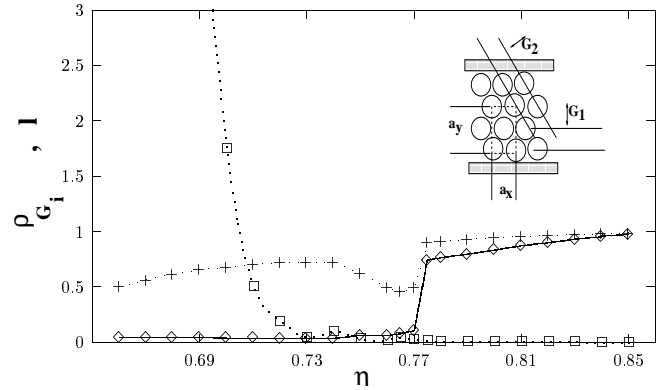


FIG. 1: Results of NVT ensemble Monte Carlo simulations of $N = n_x \times n_y = 65 \times 10$ hard disks confined between two parallel hard walls separated by a distance $L_y = 9.001 d$ where d is the hard disk diameter. Inset shows the geometry used; only four layers have been shown for clarity. The reciprocal lattice vectors (RLVs) \mathbf{G}_1 and \mathbf{G}_2 , the rectangular unit cell and the lattice parameters a_x and a_y are also shown. At $\eta = 0.85$ we have a strain free triangular lattice. Plots show $\rho_{\mathbf{G}_i}, i = 1(+), 2(\diamond)$ the structure factor for RLVs $\mathbf{G}_i(\eta)$, averaged over symmetry related directions, as a function of η . The value of η is changed by changing the length of the box L_x while keeping L_y and N fixed. For each η , the system was equilibrated over 10^6 Monte Carlo steps (MCS) and data averaged over a further 10^6 MCS. $\rho_{\mathbf{G}_1}$ is non-zero throughout implying long ranged orientational order. In contrast, $\rho_{\mathbf{G}_2}$ jumps to zero at $\eta = \eta_{c1} \approx .77$. Also plotted in the same graph is the Lindemann parameter $l(\square)$ which diverges below $\eta = \eta_{c3} = .7 < \eta_{c1}$. Note that at η_{c1} $\chi = 9.54 \approx n_l (= 10) - 1/2$. The lines in the figure are a guide to the eye.

may also be relevant for similarly confined atomic systems interacting with more complex potentials.

The bulk system of hard disks where particles i and j , in two dimensions, interact with the potential $V_{ij} = 0$ for $|\mathbf{r}_{ij}| > d$ and $V_{ij} = \infty$ for $|\mathbf{r}_{ij}| \leq d$, where d is the hard disk diameter and $\mathbf{r}_{ij} = \mathbf{r}_j - \mathbf{r}_i$ the relative posi-

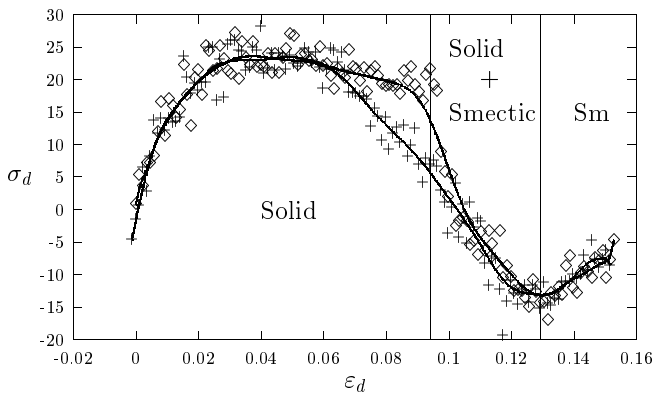


FIG. 2: A plot of the normal stress σ_d versus the conjugate strain $\varepsilon_d = (\eta_0 - \eta)/\eta_0$ ($\eta_0 = 0.85$) obtained from our Monte Carlo simulations of 65×10 hard disks showing a typical Van der Waals loop in the constant strain ensemble. Data for the plot is obtained by equilibrating at each strain value for 2×10^4 MCS and averaging the data for a further 3×10^4 MCS. The stress for the hard disk system has been calculated by the standard method[15] by averaging the collision probability. It is minimum at $\eta = \eta_{c_2} \approx .74$. The entire cycle consisting of increasing ε_d (\diamond) and again decreasing to zero (+) using typical parameters appropriate for an atomic system, corresponds to a real frequency of ≈ 100 KHz. The lines in the figure are a guide to eye. The solid ($\eta > \eta_{c_1}$), two phase ($\eta_{c_2} < \eta < \eta_{c_1}$) and smectic (Sm) ($\eta < \eta_{c_2}$) regions are indicated in the figure. We have repeated this calculation with a cycle frequency 10K Hz – 1MHz with no essential change in the results.

tion vector of the particles, has been extensively[3, 4, 6] studied. Apart from being easily accessible to theoretical treatment[11], experimental systems with nearly “hard” interactions viz. sterically stabilized colloids[13] are available. The hard disk free energy is entirely entropic in origin and the only thermodynamically relevant variable is the number density $\rho = N/V$ or the packing fraction $\eta = (\pi/4)\rho d^2$. Simulations[4], experimental[13] and theoretical[14] studies of hard disks show that for $\eta > \eta_f = .719$ the system exists as a triangular lattice which transforms to a liquid below $\eta_m = .706$. The small intervening region contains a hexatic phase predicted by the Kosterlitz-Thouless-Halperin-Nelson-Young theory[5] of two dimensional melting. The surface free energy of the hard disk system in contact with a hard wall has also been obtained[12] taking care that the dimensions of the system are compatible with a perfect (strain-free) triangular lattice. The effect of in-commensuration, though, which may routinely arise in experiments, surprisingly, have not received the attention it deserves. We attempt to address this aspect as follows.

Consider a narrow channel in two dimensions of width L_y defined by hard walls at $y = 0$ and L_y ($V_{\text{wall}}(\mathbf{r}) = 0$ for $0 < r_y < L_y$ and $= \infty$ otherwise) and length L_x with $L_x \gg L_y$. Periodic boundary conditions are assumed in

the direction x implying $x + L_x = x$. In order that the channel may accommodate n_l layers of a homogeneous, triangular lattice with lattice parameter a_0 of hard disks of diameter d , (Fig.1) one needs,

$$L_y = \frac{\sqrt{3}}{2}(n_l - 1)a_0 + d \quad (1)$$

Defining $\chi = 1 + 2(L_y - d)/\sqrt{3}a_0$, the above condition reads $\chi = \text{integer} = n_l$ and violation of Eqn.(1) implies a rectangular strain away from the reference triangular lattice of n_l layers. The lattice parameters of a centered rectangular (CR) unit cell are a_x and a_y (Fig. 1 inset). In general, for a CR lattice with given L_y we have, $a_y = 2(L_y - d)/(n_l - 1)$ and, ignoring vacancies, $a_x = 2/\rho a_y$. The normal strain $\varepsilon_d = \varepsilon_{xx} - \varepsilon_{yy}$ is then,

$$\varepsilon_d = \frac{n_l - 1}{\chi - 1} - \frac{\chi - 1}{n_l - 1}, \quad (2)$$

where the number of layers n_l is the nearest integer to χ so that ε_d has a discontinuity at half -integral values of χ . For large L_y this discontinuity and ε_d itself vanishes as $1/L_y$ for all η .

We study the effects of this strain ε_d on the hard disk triangular solid at fixed L_y large enough to accommodate a small number of layers $n_l \sim 9 - 25$. The strain ε_d is imposed by expanding the dimension of the system L_x parallel to the walls keeping L_y fixed so that $\varepsilon_d = (\eta_0 - \eta)/\eta_0$, where η_0 is the packing fraction corresponding to an unstrained triangular solid. We monitor the Lindemann parameter $l = \langle (u^x_i - u^x_j)^2 \rangle / a_x^2 + \langle (u^y_i - u^y_j)^2 \rangle / a_y^2$ where the angular brackets denote averages over configurations, i and j are nearest neighbors and u^α_i is the α -th component of the displacement of particle i from its mean position. The parameter l diverges at the melting transition [16]. We also measure the structure factor $\rho_{\mathbf{G}} = \left| \left\langle \frac{1}{N^2} \sum_{i,j=1}^N \exp(-i\mathbf{G} \cdot \mathbf{r}_{ij}) \right\rangle \right|$, for $\mathbf{G} = \pm \mathbf{G}_1(\eta)$, the reciprocal lattice vector (RLV) corresponding to the set of close-packed lattice planes of the CR lattice perpendicular to the wall, and $\pm \mathbf{G}_2(\eta)$ the four equivalent RLVs for close-packed planes at an angle ($= \pi/3$ and $2\pi/3$ in the triangular lattice) to the wall (see Fig. 1 inset).

We find, throughout, $\rho_{\mathbf{G}_2} < \rho_{\mathbf{G}_1} \neq 0$, a consequence of the hard wall constraint[12] which manifests as an oblate anisotropy of the local density peaks in the solid. As η is decreased (see Fig. 1 for details) both $\rho_{\mathbf{G}_1}$ and $\rho_{\mathbf{G}_2}$ show a jump at $\eta = \eta_{c_1}$ close to $\chi \approx n_l - 1/2$. For $\eta < \eta_{c_1}$ we get $\rho_{\mathbf{G}_2} = 0$ with $\rho_{\mathbf{G}_1} \neq 0$ signifying a transition from crystalline to smectic like order. The Lindemann parameter l remains zero and shows a divergence only below $\eta = \eta_{c_3} (\approx \eta_m)$ indicating a finite-size- broadened melting of the smectic to a modulated liquid phase. We have also calculated the normal stress $\sigma_d = \sigma_{xx} - \sigma_{yy}$ (see Fig. 2). For $\eta = \eta_0$ the stress is purely hydrostatic

with $\sigma_{xx} = \sigma_{yy}$ as expected. As η decreases, the stress increases linearly in the elastic limit, flattening out at the onset of non-linear behavior at $\eta \lesssim \eta_{c1}$. At η_{c1} , σ_d decreases and eventually becomes negative. On further decrease in η below η_{c2} (Fig. 2), σ_d approaches 0 from below thus forming a Van der Waals loop typical of the constant strain ensemble. If the strain is reversed by increasing η back to η_0 the entire stress-strain curve is traced back with no remnant stress at $\eta = \eta_0$ showing that the plastic region is reversible. As L_y is increased, η_{c1} merges with η_{c3} for $\chi \gtrsim 25$. If instead, L_x and L_y are both rescaled to keep χ fixed or periodic boundary conditions are imposed in both x and y directions, the transitions in the various quantities occur approximately simultaneously as expected in the bulk system. Varying n_x in the range 10 – 1000 produces no essential change in results.

For $\eta_{c3} < \eta < \eta_{c1}$ we observe that the smectic order appears within narrow bands (Fig. 3) which nucleate at η_{c1} . Inside these bands the number of layers is less by one and the system in this range of η is in a mixed phase. A plot (Fig.3(a)) of $\chi(x)$, obtained by averaging the instantaneous a_y from particle configurations over a strip spanning L_y , shows bands in which χ is less by one compared to the crystalline regions. Once nucleated narrow bands coalesce to form wider bands, the dynamics of which is, however, extremely slow. The bands grow as η is decreased. Calculated diffraction patterns (Fig. 3 (a)) show that, locally, within a smectic band $\rho_{\mathbf{G}_1} \gg \rho_{\mathbf{G}_2}$ in contrast to the solid region where $\rho_{\mathbf{G}_1} \approx \rho_{\mathbf{G}_2} \neq 0$.

Strong finite size corrections makes a complete theoretical treatment of this problem difficult. However, significant progress may be made using qualitative arguments as we show below. The total free energy of the system \mathcal{F}^T may be decomposed as,

$$\mathcal{F}^T(\eta, \chi) = K^\Delta(\eta) \varepsilon_a^2(\chi) + \mathcal{F}^\Delta(\eta) \quad (3)$$

where $K^\Delta(\eta)$ is an elastic constant and $\mathcal{F}^\Delta(\eta)$ the free energy of the perfect triangular lattice in contact with a hard wall[12] at packing fraction η . It is clear that \mathcal{F}^T has minima for all $\chi = n_l$. For half integral values of χ the crystalline structure is metastable with respect to an intervening smectic when adjacent local density peaks of the solid overlap in the x direction. This overlap is facilitated by the (oblate) anisotropy of the solid density peaks. For large L_y the minima in \mathcal{F}^T merge to produce a smooth free energy surface independent of χ . For small L_y all regions of the parameter space corresponding to non-integral χ are also *globally* unstable as belied by the loop in the stress-strain curve (Fig.2). The system should therefore break up into regions with various n_l . Such fluctuations are, however, suppressed due to the structure of interfaces between regions of differing n_l . A superposition of many particle positions near such an interface (see Fig. 3(b)) shows that: (1) the width of the

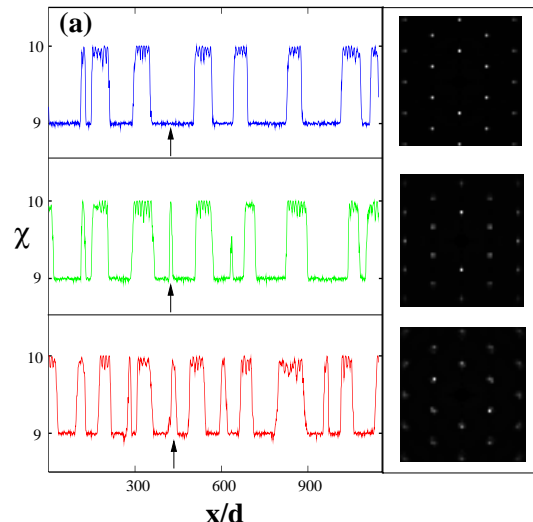


FIG. 3: (color on-line) (a) Plot of $\chi(x)$ as a function of the x/d at $\eta = .76$ after 3×10^5 , 5×10^5 and 2×10^6 (top) MCS for $N = 10^4$. Note that $\chi = 10$ in the solid and $= 9$ in the smectic regions. Arrows show the coalescence of two bands as a function of time. The panel on the right shows calculated diffraction patterns for the solid (top), smectic (middle) and inter-facial (bottom) regions. Inversion symmetry is broken at the interface because of the inter-facial dislocation (see below). (b) Close up view of a crystal-smectic interface from superimposed positions of 10^3 configurations at $\eta = .77$. The colors code the local density of points from red (high) to blue (low). Note the misfit dislocation in the inter-facial region.

interface is large, spanning about 10 – 15 atomic spacings and (2) the interface between n_l layered crystal and $n_l - 1$ layered smectic contains a *dislocation* with Burger's vector in the y direction which makes up for the difference in the number of layers. Note that the presence of these dislocations breaks inversion symmetry as observed in the local diffraction patterns. The core region of this dislocation extends over many layers with some of the disks within the interface alternating between positions corresponding to either a smectic or a solid. Each band of width s is therefore held in place by a dislocation-anti-dislocation pair (Fig. 3). In analogy with classical nucleation theory[18], the free energy F_b of a single band can be written as

$$F_b = -\Delta F s + E_c + \frac{1}{4\pi} b^2 K^\Delta \log \frac{s}{a_0} \quad (4)$$

where $b = a_y/2$ is the Burger's vector, ΔF the free energy difference between the crystal and the smectic per unit length and E_c the core energy for a dislocation pair. Bands nucleate when dislocation pairs separated by $s > \frac{1}{4\pi} b^2 K^\Delta / \Delta F$ arise due to random fluctuations. Band coalescence occurs by diffusion aided dislocation "climb" which is extremely improbable in a high density phase leading to slow kinetics. The growing smectic

bands are in a state of tension in the y direction implying $\sigma_{yy} > \sigma_{xx}$ which is countered by the compressive stress in the crystalline region. Growth of smectic bands therefore reduces σ_d which attains a minimum at $\eta = \eta_{c_2}$ when a single band spans the entire length. Subsequently $\sigma_d \rightarrow 0$, the value in the liquid phase. Since orientation relationships between the crystal and smectic are preserved, the stress-strain relationship is completely determined by the amount of the co-existing phases which explains the reversibility[19]. For large values of L_y the smectic phase vanishes since the strains involved themselves go to zero. Nevertheless, transition between n_l and $n_l \pm 1$ layered crystals have been observed by us. We must mention here that the choice of the ensemble, viz. constant strain, is crucial since, in the constant stress ensemble, the hard disk system fails at η_{c_1} and the strain diverges producing a homogeneous low density gas with no interface. Finally, our smectic bands are reminiscent of “slip” or “deformation” bands which arise during plastic flow of macroscopic ductile materials[20].

Apart from constrained hard sphere colloids[13] where our results are directly testable, strain induced crystal-smectic transition may be observable in experiments on the deformation of mono-layer atomic nano-beams or strips of real materials confined to lie within a channel[1]. This is because the constraints we choose to study are geometrical and would exist in any system. The occurrence of a smectic phase may be important for the tribological[21] properties of nano-scale machine parts where atomic friction plays an important role in their function. In the future we would like to study the kinetics of the crystal-smectic transition in detail as well as the effect of substrate disorder on the nature of this transition.

The authors thank M. Rao, V. B. Shenoy and A. Datta for useful discussions; D. C. thanks C.S.I.R., India, for a fellowship. Financial support by Department of Science and Technology, India, is gratefully acknowledged.

[1] R. Giau *et. al.*, Phys. Rev. Lett. **85**, 622 (2000); A. N. Cleland and M. L. Roukes, Appl. Phys. Lett. **69**, 2653

- (1996).
- [2] I Goldhirsh and C. Goldenberg, European Physical Journal **E 9**, 245 (2002).
- [3] B.J. Alder, T.E. Wainwright, Phys. Rev. B **127**, 359 (1962); J.A. Zollweg, G.V. Chester, P.W. Leung, Phys. Rev. B **39** 9518 (1989); H. Weber, D. Marx, Europhys. Lett. **27** 593 (1994).
- [4] A. Jaster, Physica A.**277**, 106 (2000).
- [5] J. M. Kosterlitz and Thouless, J. Phys. C **6**, 1181 (1973); D. R. Nelson and B. I. Halperin, Phys. Rev. B **19**, 2457 (1979); A. P. Young, Phys. Rev. B **19** 1855 (1979).
- [6] S. Sengupta, P. Nielaba, K. Binder, Phys. Rev. **E 61**, 6294 (2000).
- [7] S. Ostlund and B. I. Halperin Phys. Rev. B **23**, 335 (1981).
- [8] A. Chowdhury, B. J. Ackerson, N. A. Clark, Phys. Rev. Lett. **55**, 833 (1985); Q.-H. Wei, C. Bechinger, D. Rudhart and P. Leiderer, Phys. Rev. Lett. **81**, 2606 (1998).
- [9] E. Frey, D. R. Nelson and L. Radzihovsky Phys. Rev. Lett. **83**, 2977 (1999).
- [10] W. Strepp, S. Sengupta, P. Nielaba Phys. Rev. E **63**, 46106 (2001);
- [11] J. P. Hansen and I. R. MacDonald *Theory of simple liquids* (Wiley, Cluchester, 1989).
- [12] M. Heni and H. Löwen, Phys. Rev. E **60**, 7057 (1999).
- [13] I. W. Hamley *Introduction to Soft Matter: polymer, colloids, amphiphiles and liquid crystals* (Wiley, Cluchester, 2000).
- [14] V.N. Ryzhov, E.E. Tareyeva, Phys. Rev. B **51**, 8789 (1995).
- [15] O. Farago and Y. Kantor, Phys. Rev. E **61**, 2478 (2000).
- [16] K. Zahn, R. Lenke and G. Maret, Phys. Rev. Lett. **82**, 2721 (1999)
- [17] P. M. Chaikin and T. C. Lubensky *Principles of condensed matter physics*, (Cambridge University Press, 1995).
- [18] J. S. Langer in *Solids far from equilibrium*, (C. Godréche, Ed. Cambridge University Press, Cambridge, 1992).
- [19] Interestingly, reversible plastic flow has also been observed in the mechanical response of smectic vesicles where dislocations in the smectic phase play a crucial role, see for eg. T. Roopa and G. V. Shivashankar, Appl. Phys. Lett. **82**, 1631 (2003); T. Roopa, Yashodhan Hatwalne, G. V. Shivashankar and Madan Rao, preprint (2003).
- [20] R. W. Cahn and P. Haasen Eds. *Physical Metallurgy*, (North Holland, Amsterdam, 1996).
- [21] E. Barrena *et. al.*, Phys. Rev. Lett. **82**, 2880 (1999)

This figure "fig3b.jpg" is available in "jpg" format from:

<http://arxiv.org/ps/cond-mat/0401121v1>